Title
LL-37 attenuates inflammatory impairment via mTOR signaling-dependent mitochondrial protection

Authors
Sun, Wenyan
Zheng, Yan
Lu, Zhuoyang
et al.

Publication Date
2014-09-01

DOI
10.1016/j.biocel.2014.06.015

Peer reviewed

The International Journal of Biochemistry & Cell Biology 54 (2014) 26–35

Contents lists available at ScienceDirect

The International Journal of Biochemistry & Cell Biology

journal homepage: www.elsevier.com/locate/biocel

LL-37 attenuates inflammatory impairment *via* mTOR signaling-dependent mitochondrial protection

Wenyan Sun[a], Yan Zheng[b,*], Zhuoyang Lu[a], Hui Wang[a], Zhihui Feng[a], Juan Wang[b], Shengxiang Xiao[b], Feng Liu[c,d], Jiankang Liu[a,e,**]

[a] Center for Mitochondrial Biology and Medicine, The Key Laboratory of Biomedical Information Engineering of Ministry of Education, School of Life Science and Technology and Frontier Institute of Science and technology, Xi'an Jiaotong University, Xi'an 710049, China
[b] Department of Dermatology, The 2nd Affiliated Hospital of Xi'an Jiaotong University, Xi'an 710004, China
[c] Department of Medicine, University of California Irvine Medical School, Irvine, CA 92697, USA
[d] Chao Family Comprehensive Cancer Center, University of California Irvine Medical School, Irvine, CA 92697, USA
[e] Department of Pharmacology & Pharmaceutical Sciences, School of Pharmacy, University of Southern California, Los Angeles, CA 90089-9121, USA

ARTICLE INFO

Article history:
Received 5 February 2014
Received in revised form 2 June 2014
Accepted 21 June 2014
Available online 28 June 2014

Keywords:
LL-37
Mitochondrion
Inflammation
mTOR
HaCaT cells

ABSTRACT

The human cationic antimicrobial protein LL-37 is a multifunctional host defense peptide with a wide range of immunomodulatory activities. Previous work has shown that LL-37 exerts both pro- and anti-inflammatory effects. The role of mitochondria in the skin inflammatory effects of LL-37 has not been well studied. Therefore, our aim was to investigate the immunomodulatory effect of LL-37 in HaCaT cells and to delineate the underlying mechanisms related to mitochondrial function. Immunohistochemistry results from tissue microarrays showed strong cytoplasmic LL-37 staining in inflammatory cells in chronic dermatic inflammation. Using exogenous LL-37 stimulation and LL-37 knockdown and overexpression, LL-37 was demonstrated to dramatically reduce the mRNA levels and protein secretion of inflammatory cytokines including IL-6, IL-8, IL-1α and tumor necrosis factor-α (TNF-α), which are induced by lipopolysaccharides (LPS). The anti-inflammatory effects of LL-37 are dependent upon its ability to increase mitochondrial biogenesis and to maintain mitochondrial homeostasis. Furthermore, we observed that LL-37 enhances the LPS-induced phosphorylation of extracellular signal-regulated kinase (ERK1/2) and mammalian target of rapamycin (mTOR). The mTOR inhibitor rapamycin can neutralize the protective effects of LL-37 on mitochondria. In conclusion, these results suggest that high LL-37 expression levels correlate with chronic skin inflammation; mitochondrial dysfunction occurs in HaCaT cells during inflammation; and LL-37 attenuates inflammatory impairment by stimulating mitochondrial biogenesis and protecting mitochondrial function, which are dependent upon mTOR signaling. These findings provide new insights into targeting mitochondria with LL-37 to prevent skin inflammatory reactions.

1. Introduction

Mammalian skin, particularly the epidermis, is largely composed of keratinocytes and provides an essential defensive barrier against external insults (Athar, 2002). The human cationic antimicrobial protein hCAP18/LL-37 is the only human cationic cathelicidin peptide, and its C-terminal peptide, LL-37, has been shown to be multifunctional (Hancock and Diamond, 2000; Zanetti, 2004).

Previous work has demonstrated that LL-37 may exaggerate inflammatory responses and lead to disease. Excessive LL-37 is associated with rosacea and drives inflammation and abnormal blood vessel growth through cell activation mechanisms (Yamasaki et al., 2007). The high levels of LL-37 in psoriasis may also promote undesirable inflammation (Gilliet and Lande, 2008). LL-37 can

Abbreviations: EGFP, enhanced green fluorescent protein; qRT-PCR, quantitative reverse transcription PCR; LPS, lipopolysaccharides; NC-siRNA, negative control small interfering RNA; PGC-1α, PPAR-γ co-activator-1α; PPAR, peroxisome proliferator-activated receptor; ERK2, extracellular signal-regulated kinase 2; mTOR, mammalian TOR; TOR, target of rapamycin; TSC, tuberous sclerosis complex; MAPK, mitogen-activated protein kinase.

* Corresponding author. Tel.: +86 29 8266 4232.
** Corresponding author at: Center for Mitochondrial Biology and Medicine, The Key Laboratory of Biomedical Information Engineering of Ministry of Education, School of Life Science and Technology and Frontier Institute of Science and technology, Xi'an Jiaotong University, Xi'an 710049, China. Tel.: +86 29 82665849.
E-mail addresses: zenyan66@126.com (Y. Zheng), j.liu@mail.xjtu.edu.cn (J. Liu).

http://dx.doi.org/10.1016/j.biocel.2014.06.015
1357-2725/

indirectly promote the recruitment of inflammatory cells by inducing bronchial epithelial cells to release interleukin-8 (IL-8) (Filewod et al., 2009). LL-37 can also augment the secretion of IL-6 and IL-10 induced by the proinflammatory cytokine IL-1β in myeloid cells (Yu et al., 2007).

LL-37 can have opposing effects because it can also be anti-inflammatory. For example, LL-37 dramatically suppresses tumor necrosis factor α (TNF-α) production induced by the stimulation of human monocytes or macrophage cell lines with lipopolysaccharide (LPS) or lipoteichoic acid (LTA) *in vitro* (Mookherjee et al., 2006; Scott et al., 2000). LL-37 also reduces LPS and interferon γ (IFN-γ) responses in human peripheral blood mononuclear cells (PBMCs) and mouse splenic B cells (Nijnik et al., 2009). LL-37 selectively reduces proinflammatory macrophage responses (Brown et al., 2011) and inhibits dsRNA/TLR3-induced TNF-α and IL-8 in keratinocytes (Chen et al., 2013). Consistent with these suppressive effects *in vitro*, LL-37 is protective in mouse models of LPS-induced sepsis (Scott et al., 2002). In addition, LL-37 up-regulates formyl peptide receptor-like 1 (FPRL1) expression (Carretero et al., 2008) and inhibits apoptosis by activating the cyclooxygenase 2 (COX-2) pathway in HaCaT cells (Chamorro et al., 2008). LL-37 expression can be regulated by hypoxia-inducing factor 1 α (HIF-1α) (Nijnik and Hancock, 2009; Peyssonnaux et al., 2008). Therefore, the contrasting effects of LL-37 on inflammation may depend on multiple factors, including peptide concentration, processing time, and disease and cell type.

Autophagy is a crucial component of the cellular stress adaptation response (White et al., 2010), and its pathways have been demonstrated to play a key role in fine-tuning inflammatory responses in keratinocytes (Fésüs et al., 2011). Mitochondria play a central role in the initiation of inflammasomes and other inflammatory pathways (Green et al., 2011). Therefore, it is likely that the accumulation of damaged mitochondria is an important cause of inflammation. Stimulation of autophagy may mediate cytoprotective and anti-inflammatory effects, which may be at least partially ascribed to the removal of dysfunctional mitochondria (Green et al., 2011). Accumulating data have demonstrated that mammalian target of rapamycin (mTOR) regulates autophagy (Wullschleger et al., 2006). Tuberous sclerosis complex (TSC), the ribosomal p70S6 kinase (p70S6 K), and initiation factor 4E-binding protein 1 (4E-BP1) are the most extensively studied targets of mTOR (Harris and Lawrence, 2003; Inoki et al., 2002; Jacinto and Hall, 2003; Potter et al., 2002).

Consequently, we postulated that impairment of mitochondrial function by inflammatory mediators is a mechanism by which skin inflammation occurs. In the present study, we sought to understand the relationship between LL-37 and skin inflammation and to delineate the underlying mechanisms. We first applied immunohistochemistry to study LL-37 protein expression in chronic dermatic inflammation that was not psoriasis or atopic dermatitis using skin tissue microarrays (TMAs). Second, LL-37 knockdown and overexpression studies were performed in HaCaT cells. Third, the effect of exogenous LL-37 stimulation and LL-37 knockdown and overexpression on inflammatory markers, mitochondrial function, homeostasis, and autophagy were examined. Finally, the underlying mechanisms of the effects of LL-37 on signaling pathways involving extracellular signal-regulated kinase (ERK) and TSC2/mTOR were investigated.

2. Materials and methods

2.1. Antibodies and reagents

The peptide LL-37 (LLGDFFRKSKEKIGKEFKRIVQRIKDFLRNLVPRTES) was purchased from Anaspec (Fremont, CA). All other chemicals were analytical purity-grade reagents from Sigma–Aldrich (St. Louis, MO) and local vendors.

Table 1
Primers for mRNA quantitation using quantitative real-time PCR.

Forward	Reverse
TNF-α	TCCTTCAGACACCCTCAACC AGGCCCCAGTTTGAATTCTT
IL-6	AAGCCAGAGCTGTGCAGATGAGTA TGTCCTGCAGCCACTGGTTC
IL-8	GTCCTTGTTCCACTGTGCCT GCTTCCACATGTCCTCACAA
IL-1α	TGGCTCATTTTCCCTCAAAAGTTG AGAAATCGTGAAATCCGAAGTCAAG
IL-1β	CCAGGGACAGGATATGGAGCA TTCAACACGCAGGACAGGTACAG
LL-37	GGCAAGCTTGAGGCAGACATGG GCCGGATCCAGGGTAGGGAACAC
β-Actin	TGGCACCCAGCACAATGAA CTAAGTCATAGTCCGCCTAGAAGCA

2.2. TMA and immunohistochemistry

Skin TMA sections (Cybrdi, Shanxi ChaoYing, Xi'an, China), which included 80 samples (12 squamous cell carcinoma, 12 basal cell carcinoma, 12 malignant melanoma, 10 condyloma acuminatum, 6 basal cell papilloma, 1 cyst, 1 verruca vulgaris, 6 hyperplasia, 5 chronic inflammation, 5 cancer-adjacent tissue, 5 cancer-adjacent normal dermatic tissue, and 5 normal dermatic tissue) were assayed as previously described (Park et al., 2008) (Table 2). Briefly, the anti-LL-37 primary antibody (Santa Cruz Biotechnology, Santa Cruz, CA) was applied followed by the Polink-2 plus® polymer HRP detection system (Zhongshan Jinqiao, Beijing, China). Immunohistochemical staining was evaluated as described previously (Möllerström et al., 2010).

2.3. Cell culture and stable cell lines

The normal human HaCaT cell line was obtained from the Chinese Academy of Sciences (Kunming, China) and cultured in DMEM supplemented with 10% fetal calf serum. The complete LL-37 region was amplified by reverse transcription PCR from HaCaT cells using the primers shown in Table 1 and inserted into the BamHI sites of pEGFP-C3 (Clontech, Hampshire, UK), creating LL-37-EGFP. The plasmid was verified by sequence analysis to confirm the absence of mutations. The stable LL-37-EGFP and NC-EGFP HaCaT cell lines were constructed as previously described (Takeichi et al., 2010). Transfected cells were subcultured in the presence of 600 ng/ml G418 (Invitrogen, Carlsbad, CA).

2.4. Cell fixation and immunofluorescence

LL-37 and NC-EGFP HaCaT cells were cultured on coverslips, fixed with 4% paraformaldehyde (Sigma–Aldrich) for 20 min, and permeabilized with 0.1% Triton X-100/PBS. After blocking in 5% BSA/PBS, the cells were incubated with a primary antibody against LL-37 for 2 h, washed, and then incubated with the appropriately conjugated secondary antibody (Beyotime, Jiangsu, China) for 60 min. Nuclear staining was performed using 4,6-diamidino-2-phenylindole (DAPI; Sigma). Immunofluorescence was visualized using a confocal laser scanning microscope (Zeiss, Oberkochen, Germany).

2.5. siRNA directed against LL-37 expression in HaCaT cells

Three siRNA oligonucleotides targeting LL-37 and designed by GenePharma (Shanghai, China) were evaluated, and one (sense: 5′-GGAAAUCUAAAGAGAAGAUTT-3′, antisense: 5′-AUCUUCUCUUUAGAUUUCCTT-3′) that demonstrated maximum LL-37 knockdown activity in HaCaT cells (transfected for 48 h) was applied. HaCaT cells were cultured in 6-well plates to 40–50% confluence and then cultured in DMEM. The cells were transfected

Table 2
Clinicopathological features of the skin TMA specimens included in this study.

	Histologic grade *N* (*N*%)			Lymph node *N* (*N*%)		Age (years, *N*, *N*%)		Gender *N* (*N*%)		LL-37-immunopositive cell count (%)
	Well	Moderate	Poor	Negative	Positive	>60	<60	Male	Female	
Squamous cell carcinoma	4(33%)	8(67%)	0	12(100%)	0	8(67%)	4(33%)	8(67%)	4(33%)	84
Basal cell carcinoma	6(46%)	7(54%)	0	13(100%)	0	7(54%)	6(46%)	9(69%)	4(31%)	76
Malignant melanoma	1(9%)	6(55%)	4(36%)	7(64%)	4(36%)	4(36%)	7(64%)	9(82%)	2(18%)	98
Condyloma acuminatum	–	–	–	–	–	0	10(100%)	1(10%)	9(90%)	54
Basal cell papilloma	–	–	–	–	–	4(67%)	2(33%)	5(83%)	1(17%)	48
Verruca vulgaris	–	–	–	–	–	0	1(100%)	1(100%)	0	35
Hyperplasia	–	–	–	–	–	2(33%)	4(67%)	4(67%)	2(33%)	89
Chronic inflammation	–	–	–	–	–	4(80%)	1(20%)	3	2	92
Cancer-adjacent tissue	–	–	–	–	–	3(60%)	2(40%)	4(80%)	1(20%)	42
Cancer-adjacent normal tissue	–	–	–	–	–	0	5(100%)	1(20%)	4(80%)	23
Normal tissue	–	–	–	–	–	0	5(100%)	3(60%)	2(40%)	17

with the LL-37-siRNA or NC-siRNA using Lipofectamine 2000 according to the manufacturer's instructions.

2.6. JC-1 assay for mitochondrial membrane potential ($\Delta\Psi$)

$\Delta\Psi$ was assessed as previously described (Feng et al., 2011). Briefly, cells were incubated with 5 μmol/L 5,5′,6,6′-tetrachloro-1,1′,3,3′-tetraethylbenzimidazolyl-carbocyanine iodide (JC-1) (Invitrogen) at 37 °C for 60 min. The fluorescence-labeled cells were washed with PBS and analyzed on a microplate fluorometer (Fluoroskan Ascent; Thermo Fisher Scientific, Waltham, MA, USA) at 488 nm excitation and 535 and 590 nm emission to measure green and red JC-1 fluorescence, respectively. The ratio of fluorescence at 590 nm *versus* 535 nm emission was used for quantitating $\Delta\Psi$.

2.7. RNA isolation and quantitative reverse transcription PCR

Quantitative PCR was performed as previously described (Hao et al., 2010). Total RNA was extracted using TRIzol reagent (Invitrogen), and reverse transcription was performed using a Takara RNA PCR kit (Takara, Dalian, China) following the manufacturer's instructions. Quantitative PCR was performed using SYBR Green Premix Ex Taq (Takara) on a real-time PCR system (Eppendorf, Germany). The relative expression ratio was calculated using the $2^{-\Delta\Delta CT}$ method. The specific primers, which were synthesized by Baiaoke Biotech (Beijing, China), are shown in Table 1.

2.8. ELISA for cytokines

TNF-α, IL-6, IL-8, IL-1α, and IL-1β levels in culture supernatants were measured using an ELISA kit purchased from Excell Biology, Inc. (Shanghai, China). Briefly, supernatants were added to 96-well plates coated with a specific monoclonal antibody. After exposure to medium, the assay plates were sequentially exposed to biotin-conjugated anti-cytokine antibodies and detected with a streptavidin-peroxidase-conjugated anti-rabbit antibody. The plate was developed using a 3,3′,5,5′tetramethylbenzidine (TMB) and the optical density of each well was determined at 450 nm on a microplate reader (Bio-Rad, Hercules, CA).

2.9. Western blot assays

Western blots were performed as previously described (Feng et al., 2011). Briefly, blocked membranes were incubated with anti-PGC-1α, anti-Mfn1, anti-Mfn2, anti-DRP1, anti-β-actin, or anti-α-tubulin (Santa Cruz); anti-OPA1 (BD Biosciences, San Jose, CA); anti-OxPhos Complex I, anti-OxPhos Complex II, anti-OxPhos Complex III or anti-Complex V (Invitrogen); anti-LL-37 (Abgent, San Diego, CA); or anti-Beclin1, anti-LC3B, anti-Atg 7, anti-mTOR, anti-p-mTOR (Ser2448), anti-p-ERK1/2 (Thr202/Tyr204) or anti-ERK2 (Cell Signaling Technology, Beverly, MA) at a dilution of 1:1000 or 1:2000 followed by chemiluminescent ECL detection (Pierce, Rockford, IL).

2.10. Statistical analysis

All data are representative of at least three independent experiments. Data are presented as means ± S.D. Statistical significance was calculated with GraphPad Prism 5 statistical software, with P values <0.05 considered significant.

3. Results

3.1. High levels of LL-37 protein expression in chronic dermatic inflammation and hyperplasia of dermatic tissue of squamous epithelium

Skin TMAs were used to compare the expression levels of LL-37. One case missed TMA processing and was excluded. A total of 79 cases were analyzed.

Immunohistochemical results showed that in 5 cases of chronic dermatic inflammation and 6 cases of hyperplasia of dermatic tissue of squamous epithelium, Positive LL-37 peptide shows as claybank particles which were mainly distributed in the cytoplasm in epidermal cells and inflammatory cells (Fig. 1A and B). In the epidermal layer, LL-37 was mainly localized to the stratum spinosum, whereas in the dermal layer, LL-37 was mainly expressed in inflammatory cells and vascular endothelial cells. In 5 cases of normal dermatic tissue that was not adjacent to cancer sites and 5 cases of cancer-adjacent normal dermatic tissue, LL-37 was mainly expressed in the epidermal stratum corneum. In both cases, the protein was primarily localized to the cytoplasm (Fig. 1C and D). Inflammatory cells from chronic dermatic inflammation and hyperplasia of dermatic tissue of squamous epithelium exhibited significantly enhanced staining for LL-37 compared with samples from non-cancer-adjacent normal dermatic tissue and cancer-adjacent normal dermatic tissue ($P < 0.05$). Furthermore, we observed that in squamous cell carcinoma, basal cell carcinoma, and malignant melanoma, LL-37 expression was mainly cytoplasmic and significantly increased compared with non-cancer-adjacent normal dermatic tissue or cancer-adjacent normal dermatic tissue ($P < 0.05$, supplementary Fig. 1).

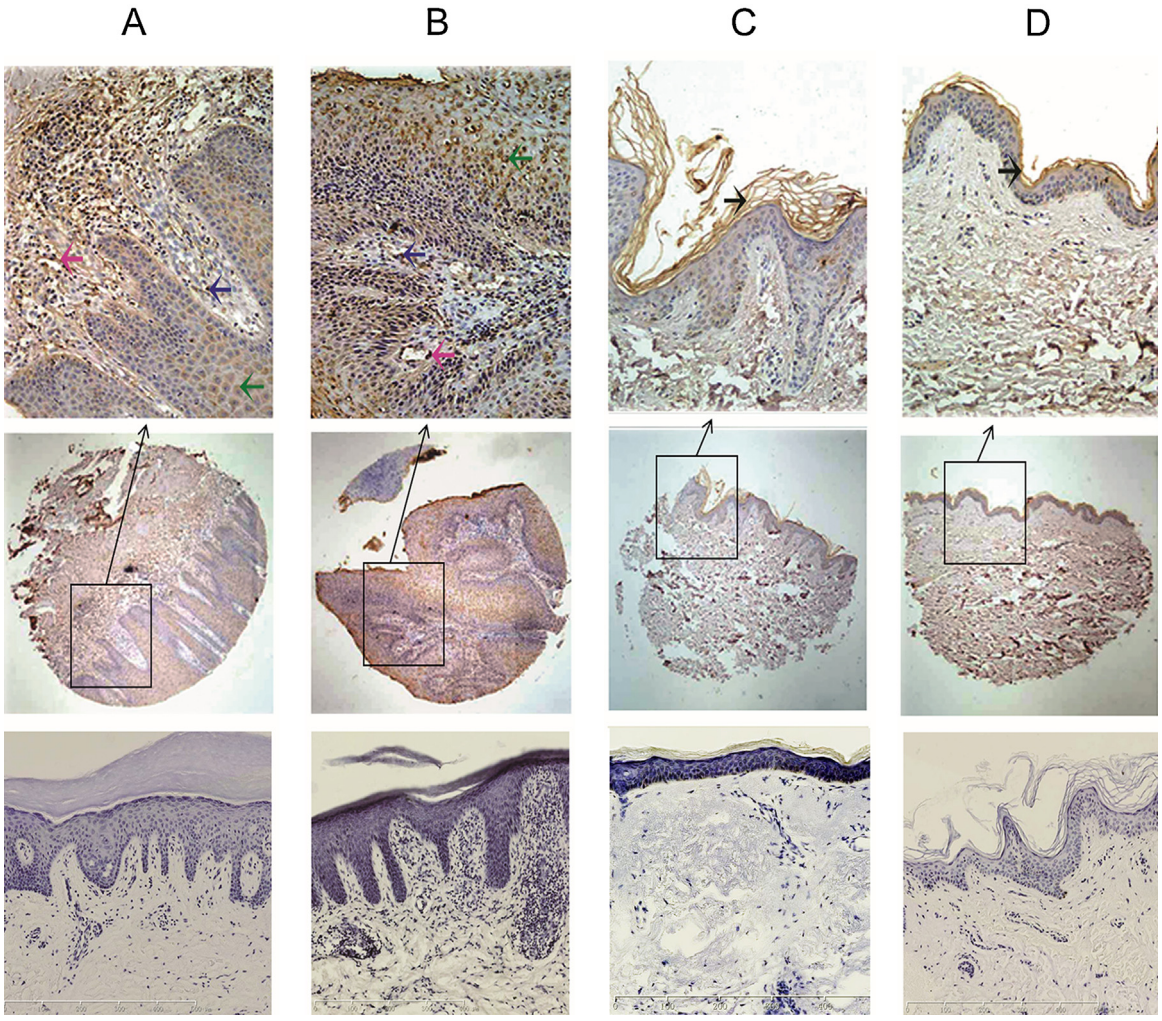

Fig. 1. Representative samples of human cationic antimicrobial protein (hCAP18/LL-37) immunohistochemical staining. Positive LL-37 peptide shows as claybank particles which were distributed in the cytoplasm in epidermal cells (green arrow) and inflammatory cells (blue arrow) and vascular endothelial cells (pink arrow) in hyperplasia of dermatic tissue of squamous epithelium (A) and chronic dermatic inflammation (B) and mainly observed in epidermal stratum corneum (black arrow) in non-cancer-adjacent normal dermatic tissue (C) and cancer-adjacent normal dermatic tissue (D). The bottom row of the images are negative control each. The data shown are representative of five or six independent experiments. Magnification 200× (upper panels) and 40× (middle panels). (For interpretation of the references to color in this figure legend, the reader is referred to the web version of this article.)

3.2. Characterization of LL-37 knockdown and overexpression in HaCaT cells

To investigate the function of LL-37 in dermatic tissue, a small interfering RNA (siRNA) against human LL-37 was used to knock down LL-37 expression; the level of LL-37 mRNA was measured 48 h later in immortalized human epithelial HaCaT cells. Compared with the negative control (NC) siRNA and non-transfected HaCaT cells, a significant decrease in LL-37 mRNA levels after LL-37-siRNA transfection was observed (Fig. 2A). In addition, HaCaT cells constitutively expressing LL-37 (LL-37-enhanced green fluorescent protein (EGFP) cells) or EGFP alone (NC-EGFP cells) were generated. LL-37 mRNA was more abundant in LL-37-EGFP HaCaT cells than in non-transfected HaCaT cells or NC-EGFP cells as determined by quantitative RT-PCR (Fig. 2B). Consistent with LL-37 mRNA overexpression, western blots and immunofluorescent staining demonstrated that the LL-37 signal from LL-37-EGFP HaCaT cells was enhanced compared with NC-EGFP cells (Fig. 2C and D).

3.3. LL-37 functionally suppresses inflammatory cytokine expression

To determine the function of LL-37 in the inflammatory response, LPS was used to induce an inflammatory response, and LL-37 levels were monitored in a dose-dependent manner. As shown in Fig. 3A and B, 24 h after exposure to LPS, HaCaT cells exhibited marked inflammatory responses as evidenced by increases in the inflammatory markers TNF-α, IL-8, and IL-1α measured by quantitative RT- PCR and enzyme-linked immunosorbent assay (ELISA). LL-37 (1.1 μM) treatment attenuated IL-8, TNF-α, and IL-1α production. A high dose of LL-37 (2.2 μM) reduced the expression of inflammatory cytokines in the presence of 100 ng/ml LPS.

Silencing LL-37 led to further increases in TNF-α, IL-8, and IL-6 mRNA and protein accumulation after LPS stimulation (Fig. 3C and D). Next, the effect of LL-37 overexpression on the expression of inflammatory cytokines was analyzed. LL-37-EGFP cells exhibited lower levels of inflammatory cytokine expression at both the mRNA and protein levels compared with the control NC-EGFP

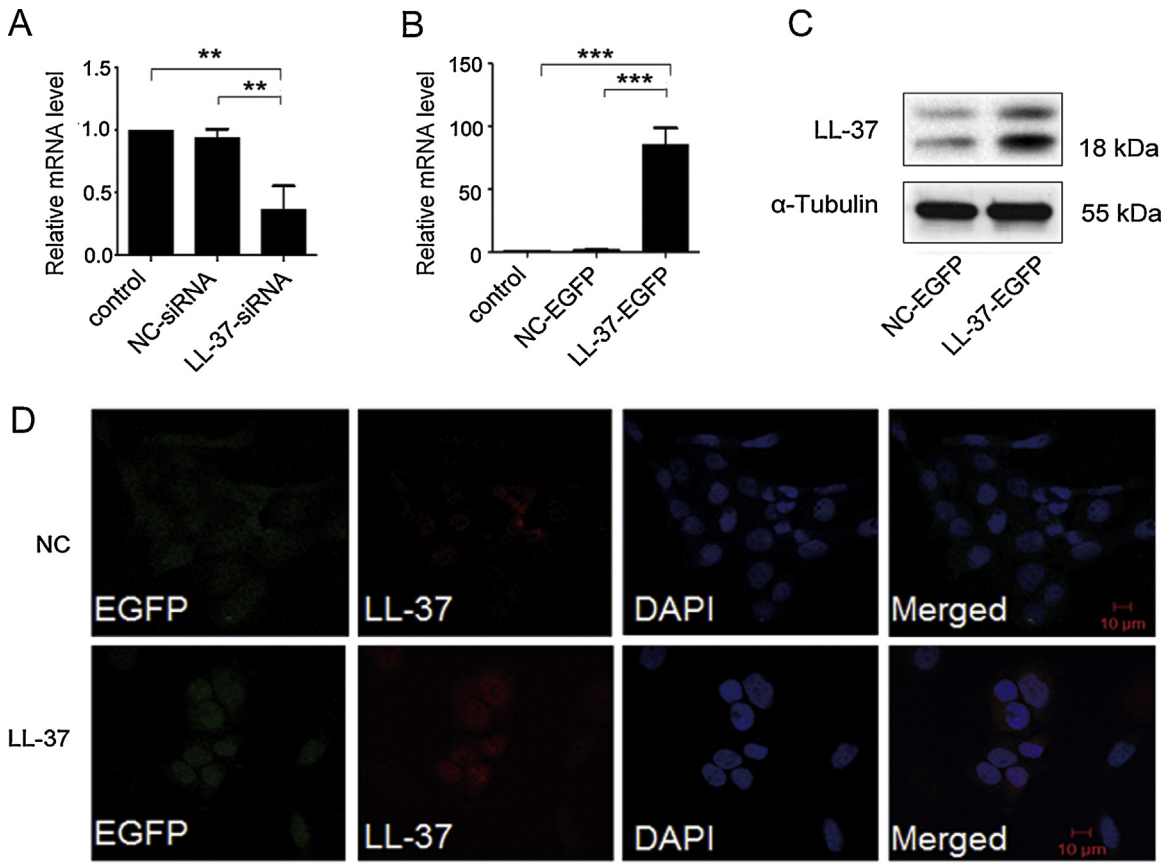

Fig. 2. Expression of LL-37 in transfected cells. (A) LL-37 mRNA levels in HaCaT cells transfected with the LL-37 small interfering RNA (siRNA) or NC-siRNA for 48 h using quantitative reverse transcription PCR (qRT-PCR). (B) LL-37 mRNA levels and (C) protein expression in LL-37-overexpressing HaCaT cells. LL-37 mRNA is normalized to α-tubulin. Error bars represent SD. $^{**}P < 0.05$ and $^{***}P < 0.001$. (D) Immunofluorescence analysis of LL-37 overexpression. Cells were stained for enhanced green fluorescent protein (EGFP) (green) and anti-LL-37 (red), and the nuclei were stained with 4,6-diamidino-2-phenylindole (DAPI) (blue). The data shown are representative of three independent experiments. (For interpretation of the references to colour in this figure legend, the reader is referred to the web version of this article.)

cells (Fig. 3E and F), suggesting a protective role of LL-37 against inflammation.

3.4. LL-37 increases mitochondrial function and regulates mitochondrial homeostasis during inflammation

Recent studies have revealed that mitochondrial dysfunction plays a key role in the inflammatory response (Cordero et al., 2013; Joven, 2013). To investigate the effect of LL-37 on mitochondrial function, the protein levels of peroxisome proliferator-activated receptor gamma coactivator-1 α (PGC-1α), the key regulator of mitochondrial biogenesis, and mitochondrial respiratory chain enzyme complexes were determined in LL-37 overexpressing and knockdown cells. As expected, LPS induced the loss of accumulation of complexes II, III and V; however, pretreatment with 1.1 or 2.2 μM LL-37 efficiently prevented these losses (Fig. 4A and B). Unlike the protein levels of complexes II, III, and V, complex I and IV levels were unaffected by LL-37 pretreatment (data not shown).

Knockdown of LL-37 and the addition of LPS to LL-37 knockdown cells led to a significant inhibition of the expression of complexes I, II, and V compared with NC-siRNA cells (Fig. 4C and D). Conversely, LL-37 overexpression led to the increased expression of PGC-1α and complexes I and V compared with empty vector control cells (Fig. 4E and F).

In addition to regulating the mitochondrial biogenesis of PGC-1α and respiratory chain enzyme complexes, mitochondrial fusion and fission are important processes that result in the continuous remodeling of mitochondrial network dynamics (Bo et al., 2010). In this study, we further found that LL-37 pretreatment or overexpression significantly inhibited the LPS-induced increase in the mitochondrial fusion-related proteins Mfn2 and OPA1 and the mitochondrial fission-related protein DRP1 (Fig. 4A, B, E and F). Upon LPS stimulation, LL-37 knockdown led to increases in the expression of Mfn2 and DRP1 (Fig. 4C and D). Therefore, we confirmed that LL-37 can regulate mitochondrial metabolism in HaCaT cells *via* various mechanisms.

3.5. LL-37 down-regulates the expression of autophagy-related proteins

Dysfunctional mitochondria are usually eliminated by autophagy, allowing cells to maintain healthy mitochondrial metabolism (Wang and Klionsky, 2011). Next, we examined the function of LL-37 in regulating autophagy. Treating HaCaT cells with LPS alone significantly increased the endogenous accumulation of Beclin1 and LC3B. Pretreatment with LL-37 dramatically inhibited LPS-induced Beclin1 and LC3B accumulation (Fig. 5A and B). These data partially confirm findings from previous studies that have demonstrated that treating HaCaT cells with LPS robustly increases punctate LC3 expression and LC3-II band intensities (Lee et al., 2011).

Additionally, transfecting HaCaT cells with an LL-37-specific siRNA dramatically increased LPS-induced Beclin1 and LC3B expression (Fig. 5C and D). In contrast, upon LPS stimulation, LL-37-overexpressing cells showed decreases in LC3B and Atg7 compared with the control NC-EGFP cells (Fig. 5E and F). These results suggest

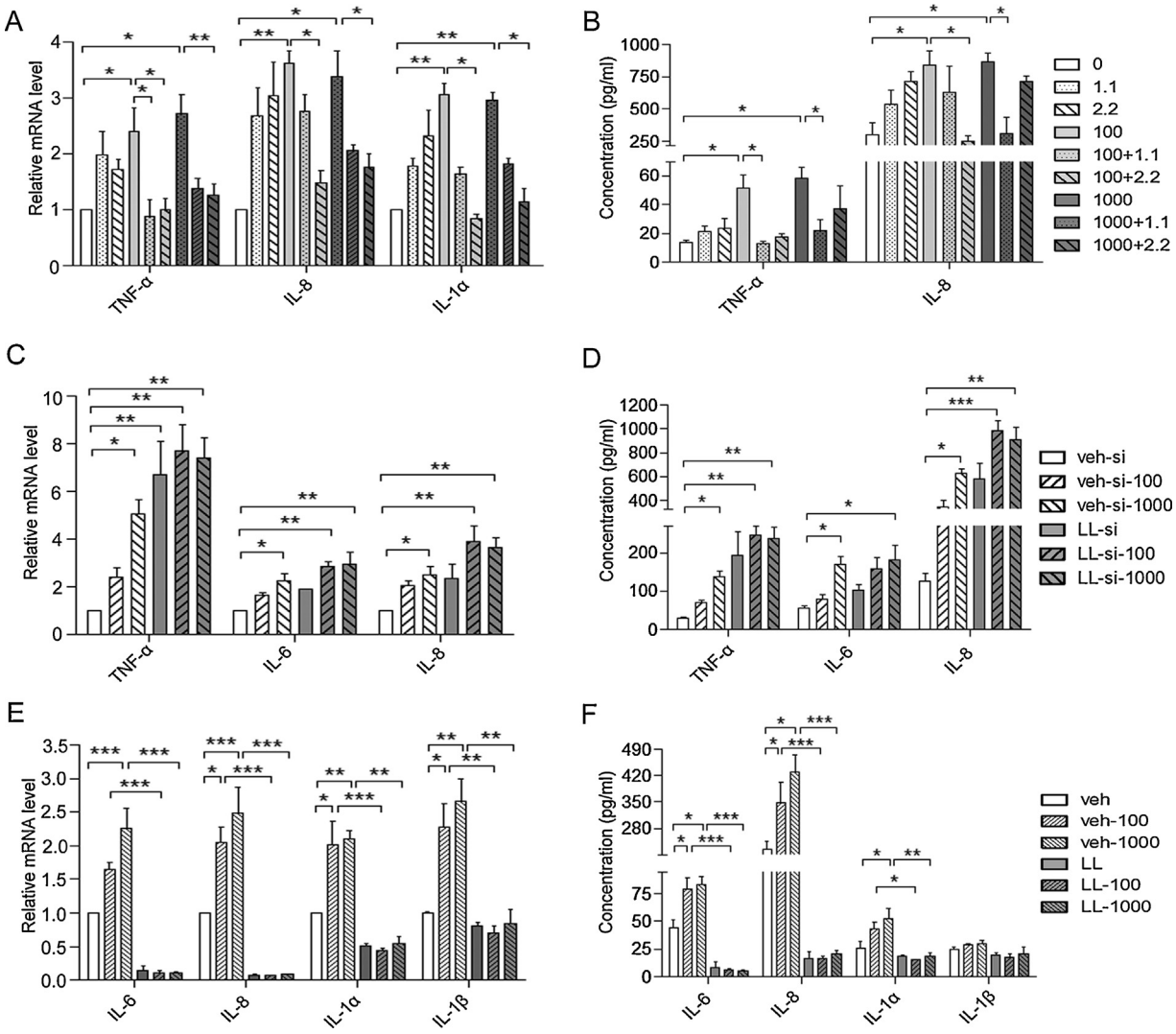

Fig. 3. Effect of exogenous LL-37 administration, LL-37 knockdown and overexpression on the lipopolysaccharide (LPS)-induced mRNA and protein expression of inflammatory cytokines using qRT-PCR and enzyme-linked immunosorbent assay (ELISA). (A, B) HaCaT cells were exposed to LPS for 24 h after preincubation with or without LL-37 for 24 h. (C, D) HaCaT cells were treated with LPS for 24 h after transfection with an LL-37 siRNA or NC-siRNA for 48 h. (E, F) Stable HaCaT cells were exposed to LPS for 24 h. Error bars represent SD. $^{*}P < 0.05$, $^{**}P < 0.01$ and $^{***}P < 0.001$. 0, control; 1.1 or 2.2, control with 1.1 or 2.2 μM LL-37, respectively; 100 or 1000, control with 100 or 1000 ng/ml LPS treatment, respectively; 100 + 1.1 or 100 + 2.2, control with 100 ng/ml LPS after preincubation with 1.1 or 2.2 μM LL-37, respectively; 1000 + 1.1 or 1000 + 2.2, control with 1000 ng/ml LPS after preincubation with 1.1 or 2.2 μM LL-37, respectively; veh-si, vehicle-siRNA; veh-si-100 or veh-si-1000, vehicle-siRNA cells with 100 or 1000 ng/ml LPS treatment, respectively; LL-si, LL-37-siRNA; LL-si-100 or LL-si-1000: LL-37-siRNA HaCaT cells with 100 or 1000 ng/ml LPS treatment, respectively; veh, vehicle; veh-100 or veh-1000, vehicle with 100 or 1000 ng/ml LPS treatment, respectively; LL, LL-37; LL-100 or LL-1000, LL-37-EGFP HaCaT cells with 100 or 1000 ng/ml LPS treatment, respectively.

that LL-37 attenuates the increased autophagy caused by inflammatory responses.

3.6. Neutralized LL-37 protects against the LPS-induced decrease in $\Delta\Psi$ via enhancement of mTOR activation

To further understand the signaling pathways upstream of the LL-37 effect, we examined a potential role for LL-37 in LPS-induced ERK and mTOR activation. LL-37 pretreatment enhanced LPS-induced ERK and mTOR activation in HaCaT cells (Fig. 6A and B). LL-37 overexpression led to higher levels of ERK and mTOR activation in LL-37-EGFP HaCaT cells after LPS stimulation compared with NC-EGFP cells (Fig. 6E and F). LL-37 knockdown consistently inhibited the phosphorylation of ERK and mTOR (Fig. 6C and D).

The ERK inhibitor U0126 and the mTOR inhibitor rapamycin were added to cells treated with exogenous LL-37 or cells overexpressing LL-37. We found that both U0126 and rapamycin decreased LPS-induced ERK and mTOR phosphorylation (Fig. 6A, B, E and F). Because inflammation induces mitochondrial dysfunction *in vitro* and *in vivo* (Hunter et al., 2007) and $\Delta\Psi$ is an important index of mitochondrial function, the effects of U0126 and rapamycin on the LL-37-mediated protection of $\Delta\Psi$ in LPS-induced inflammatory response were examined. Rapamycin and LL-37 siRNA but not the ERK inhibitor U0126 neutralized the protective effects of LL-37 and produced a low $\Delta\Psi$ (Fig. 6G–I), indicating that mTOR activation may play an essential role in LL-37-mediated protection against LPS-induced mitochondrial dysfunction.

4. Discussion

The role of LL-37 has been widely studied in two skin pathologies, atopic dermatitis and psoriasis. Patients with psoriasis express higher levels of LL-37 (Ong et al., 2002) compared with patients with atopic dermatitis. Dombrowski et al. (2011) demonstrated that intracellular LL-37 serves as an anti-inflammatory agent by blocking the DNA-triggered formation of AIM2 inflammasomes in

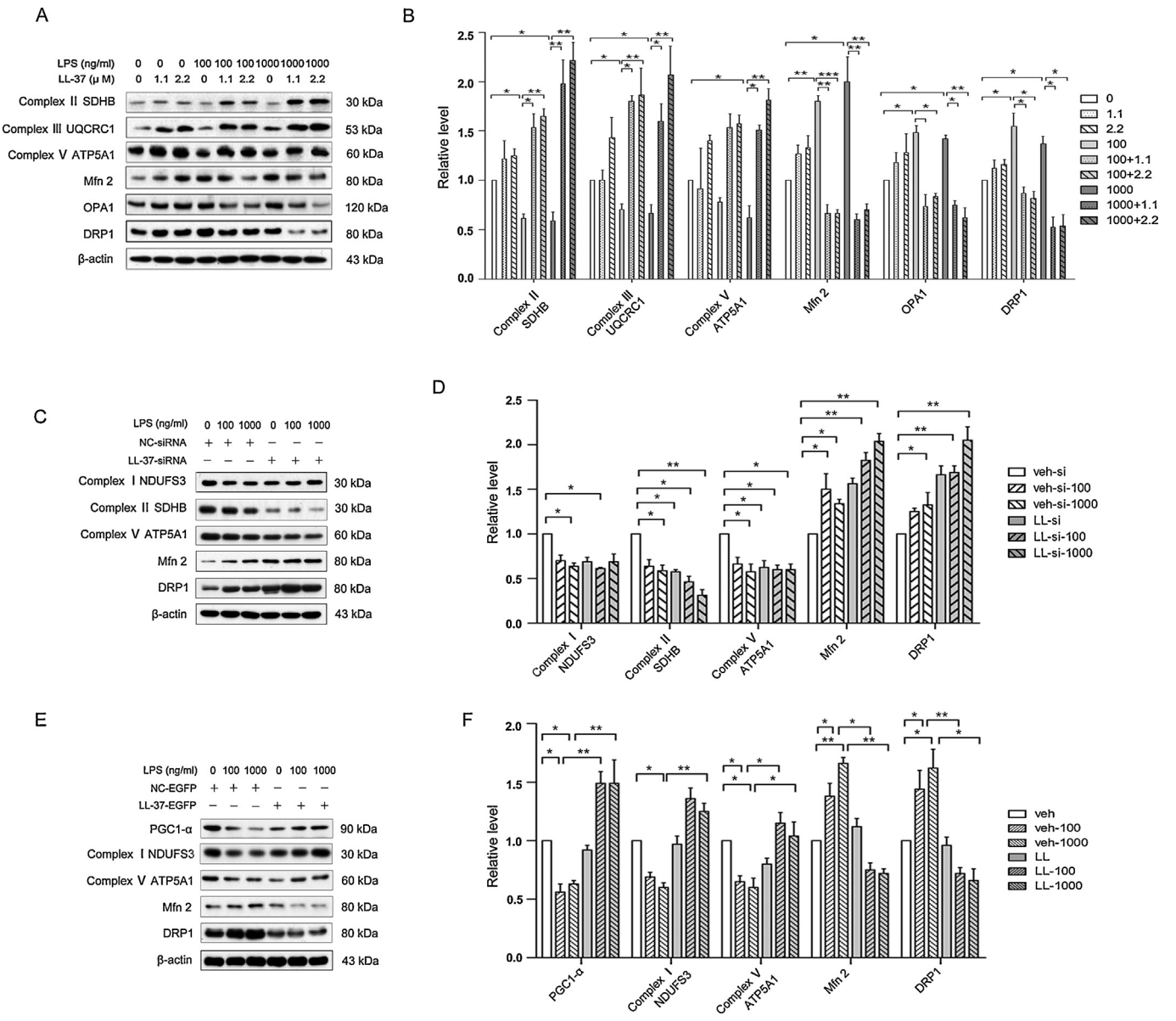

Fig. 4. Production of mitochondrial biogenesis and fusion/fission proteins in LL-37 exogenous addition, LL-37 knockdown or LL-37-overexpressing HaCaT cells. (A, B) HaCaT cells were exposed to LPS for 24 h after preincubation with or without LL-37 for 24 h. (C, D) HaCaT cells were treated with LPS for 24 h after transfection with an LL-37 siRNA or NC-siRNA for 48 h. (E, F) Stable HaCaT cells (LL-37-EGFP or NC-EGFP) were exposed to LPS for 24 h. β-actin was used as an internal loading control for cell lysates in Western blot analyses. The data shown are representative of three independent experiments. PGC-1α, PPAR-γ co-activator-1α; PPAR, peroxisome proliferator-activated receptor.

keratinocytes, inhibiting IL-1β release. However, several studies have shown that extracellular or endosomal LL-37 enhances TLR9 expression and function in keratinocytes, leading to increased IFN-α/β production (Morizane et al., 2012). Therefore, understanding the mechanisms that suppress the inflammatory response during skin inflammation may help identify therapeutic targets for treatments that are relevant to multiple inflammatory skin diseases.

In this study, skin TMAs showed that the samples from chronic dermatic inflammation and hyperplasia of dermatic tissue of squamous epithelium had much more intense staining for LL-37 than samples from normal dermatic tissue or cancer-adjacent normal dermatic tissue using immunohistochemistry. We conclude that high LL-37 levels may correlate with chronic skin inflammation. Next, plasmid DNA or siRNA approaches were used to overexpress or knock down the LL-37 gene in HaCaT cells. LL-37 administration or overexpression robustly inhibited inflammatory cytokine secretion during LPS-induced inflammation and demonstrated that LL-37 may exert anti-inflammatory effects. Therefore, LL-37 knockdown led to an increase in TNF-a, IL-8, and IL-6 mRNA and protein accumulation in the absence of LPS and further increased proinflammatory cytokine production in the presence of LPS.

Mitochondrial damage implies a direct cause-and-effect relationship between inflammation and autophagy. The selective degradation of mitochondria is termed mitophagy (Kim et al., 2007). This type of selective process is thought to play a crucial role in mitochondrial homeostasis. We found that LL-37 protected mitochondrial function and maintained mitochondrial homeostasis through regulated mitochondrial fusion and fission during LPS-induced inflammation.

In many instances, autophagy controls inflammasome activation and can limit the production of the inflammatory cytokines IL-1β and IL-18 (Saitoh et al., 2008). Autophagy can also inhibit NLRP3 activation by removing ROS-producing mitochondria (Nakahira et al., 2011; Zhou et al., 2011). In this study, LL-37

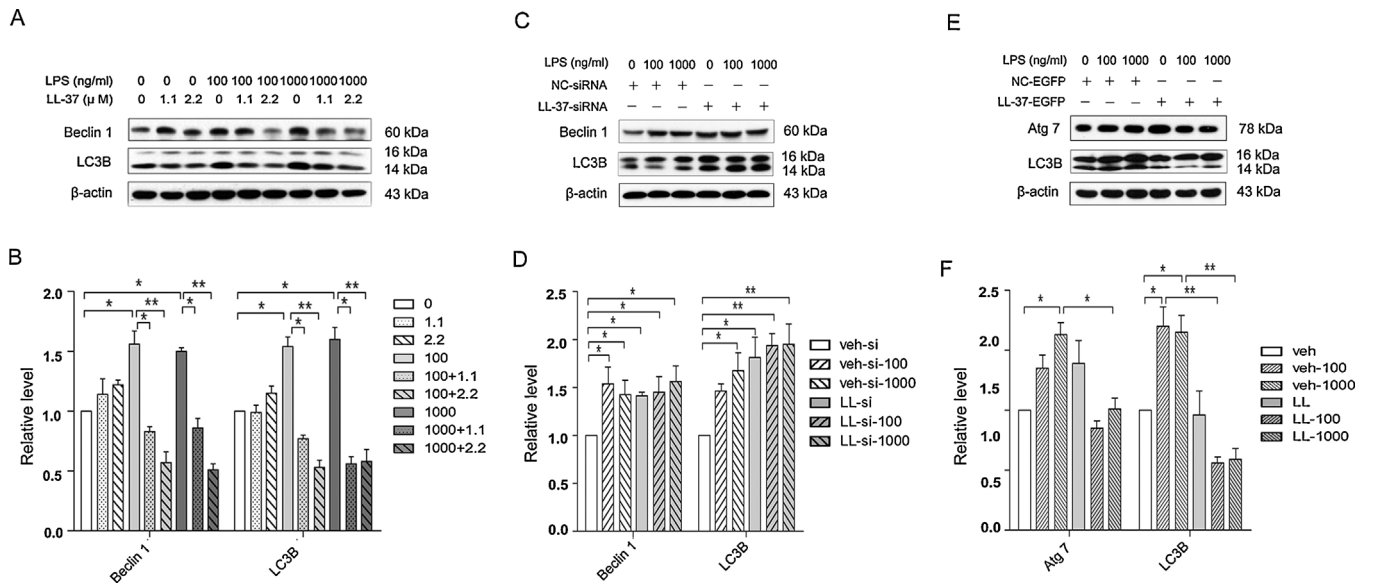

Fig. 5. Production of Beclin1, LC3B and Atg7 proteins in LL-37 exogenous addition, LL-37 knockdown or LL-37-overexpressing HaCaT cells. (A, B) HaCaT cells were exposed to LPS for 24 h after preincubation with or without LL-37 for 24 h. (C, D) HaCaT cells were treated with LPS for 24 h after transfection with an LL-37 siRNA or NC-siRNA for 48 h. (E, F) Stable HaCaT cells (LL-37-EGFP or NC-EGFP) were exposed to LPS for 24 h. The data shown are representative of three independent experiments.

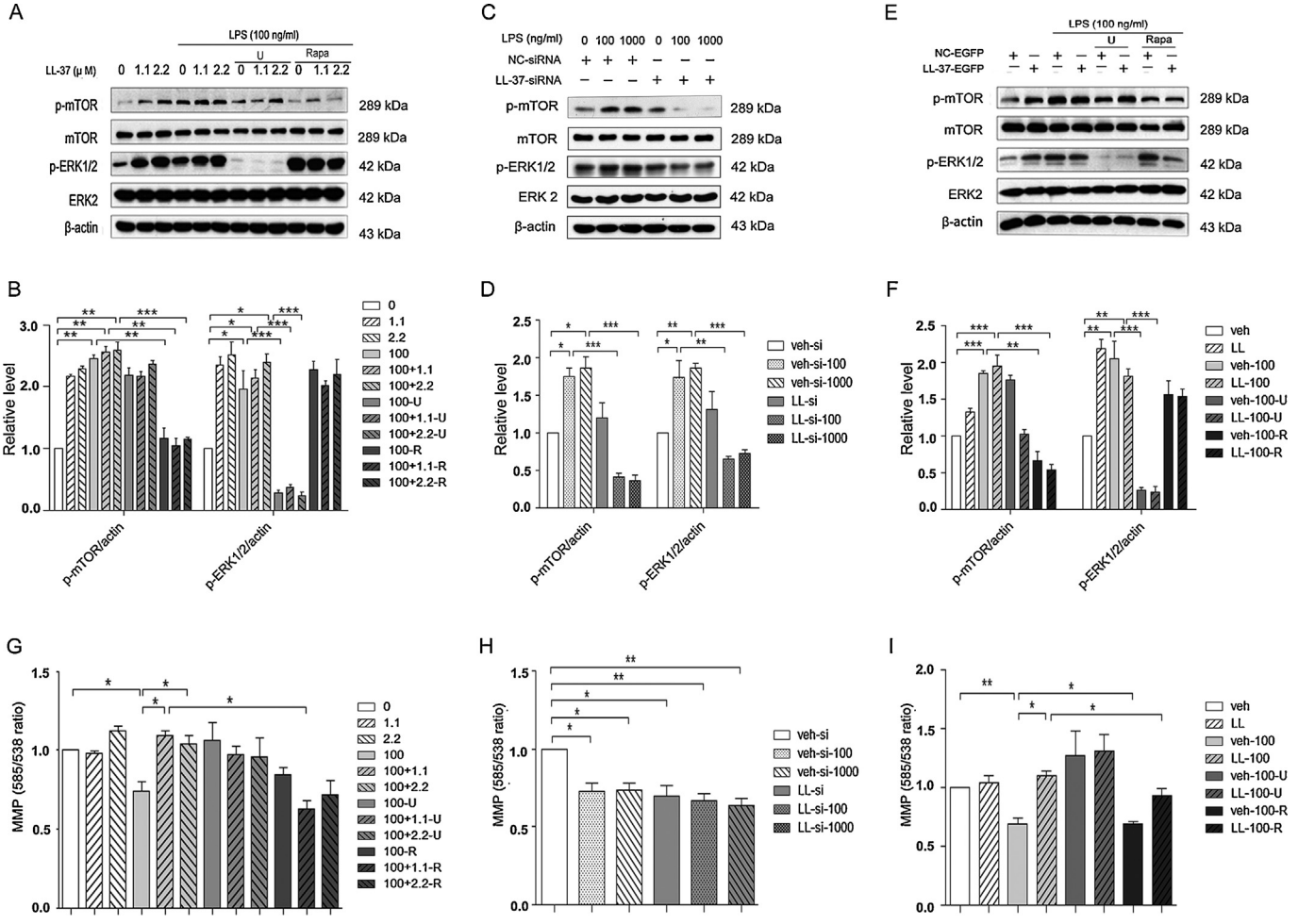

Fig. 6. LL-37 protects against LPS-induced decreases in mitochondrial membrane potential ($\Delta\Psi$) *via* enhancement of mammalian target of rapamycin (mTOR) activation. (A, B and G) HaCaT cells were pretreaed with the ERK inhibitor U0126 (*U*, 100 μM) or mTOR inhibitor rapamycin (Rapa, 100 nM) for 1 h with LPS for 24 h after preincubation with or without LL-37 for 24 h. (C, D and H) HaCaT cells were treated with LPS for 24 h after transfection with an LL-37 siRNA or NC-siRNA for 48 h. (E, F and I) Stable HaCaT cells were pretreaed with U0126 or rapamycin for 1 h after exposure to LPS for 24 h. Error bars represent SD. $^{*}P < 0.05$, $^{**}P < 0.01$, $^{\hat{}}P < 0.05$, $^{\%}P < 0.05$ and $^{\#}P < 0.05$.

administration or overexpression significantly inhibited the expression of autophagy-related proteins, and LL-37 knockdown increased during LPS-induced inflammation, which is consistent with the result that autophagy negatively regulates inflammation.

Previous studies have unraveled the TSC2-mTOR signaling pathway in limiting the proinflammatory cytokine production induced by various bacterial stimuli in monocytes, macrophages and primary dendritic cells (Weichhart et al., 2008). Mitogen-activated protein kinases (MAPKs) are implicated in inflammatory signaling, which facilitates the production of inflammatory mediators (Kaminska, 2005). ERK may modulate mTOR signaling and contribute to disease progression through the phosphorylation and inactivation of TSC2 (Ma et al., 2005). To understand the molecular mechanism of the protective effect of LL-37 in LPS-treated HaCaT cells, we analyzed the ERK and mTOR signaling pathways. We found that ERK and mTOR activation were involved after LPS stimulation and that LL-37 pretreatment and overexpression enhanced LPS-induced ERK and mTOR activation in HaCaT cells. The mTOR inhibitor, but not the ERK inhibitor, neutralized the protective effects of LL-37 against LPS, suggesting that mTOR signaling activation is necessary for LL-37's protective effects against LPS-induced inflammation and mitochondrial dysfunction.

Therefore, we have shed light on the high expression levels of LL-37 that correlate with chronic dermatic inflammation and how LL-37 may protect mitochondrial function and mitochondrial homeostasis mechanisms through mTOR signaling in skin inflammation. Moreover, we have identified and provided new insights into how mitochondria can be targeted to prevent skin inflammation.

Conflicts of interest

The authors declare no conflict of interest.

Acknowledgements

This work was supported by the National Natural Science Foundation of China (81371732) and by projects 985 and 211 of Xi'an Jiaotong University and was partially supported by New Century Excellent Talents in University and the Fundamental Research Funds for the Central Universities and for Changjiang Scholars and Innovative Research Team in University (PCSIRT:1171).

Appendix A. Supplementary data

Supplementary data associated with this article can be found, in the online version, at http://dx.doi.org/10.1016/j.biocel.2014.06.015.

References

Athar M. Oxidative stress and experimental carcinogenesis. Indian J Exp Biol 2002;40:656–67.
Bo H, Zhang Y, Ji LL. Redefining the role of mitochondria in exercise: a dynamic remodeling. In: Wei YH, Tzeng CR, Lee HM, editors. Mitochondrial research in translational medicine. Malden: Wiley-Blackwell; 2010. p. 121–8.
Brown KL, Poon GFT, Birkenhead D, Pena OM, Falsafi R, Dahlgren C, et al. Host defense peptide LL-37 selectively reduces proinflammatory macrophage responses. J Immunol 2011;186:5497–505.
Carretero M, Escamez MJ, Garcia M, Duarte B, Holguin A, Retamosa L, et al. In vitro and in vivo wound healing-promoting activities of human cathelicidin LL-37. J Investig Dermatol 2008;128:223–36.
Chamorro CI, Weber G, Grönberg A, Pivarcsi A, Ståhle M. The human antimicrobial peptide LL-37 suppresses apoptosis in keratinocytes. J Investig Dermatol 2008;129:937–44.
Chen X, Takai T, Xie Y, Niyonsaba F, Okumura K, Ogawa H. Human antimicrobial peptide LL-37 modulates proinflammatory responses induced by cytokine milieus and double-stranded RNA in human keratinocytes. Biochem Biophys Res Commun 2013;433:532–7.
Cordero MD, Díaz-Parrado E, Carrión AM, Alfonsi S, Sánchez-Alcazar JA, Bullón P, et al. Is inflammation a mitochondrial dysfunction-dependent event in Fibromyalgia? Antioxid Redox Signal 2013;18:800–7.
Dombrowski Y, Peric M, Koglin S, Kammerbauer C, Goss C, Anz D, et al. Cytosolic DNA triggers inflammasome activation in keratinocytes in psoriatic lesions. Sci Transl Med 2011:2011.
Fésüs L, Demény MÁ, Petrovski G. Autophagy shapes inflammation. Antioxid Redox Signal 2011;14:2233–43.
Feng Z, Bai L, Yan J, Li Y, Shen W, Wang Y, et al. Mitochondrial dynamic remodeling in strenuous exercise-induced muscle and mitochondrial dysfunction: regulatory effects of hydroxytyrosol. Free Radic Biol Med 2011;50:1437–46.
Filewod NCJ, Pistolic J, Hancock REW. Low concentrations of LL-37 alter IL-8 production by keratinocytes and bronchial epithelial cells in response to proinflammatory stimuli. Fems Immunol Med Microbiol 2009;56:233–40.
Gilliet M, Lande R. Antimicrobial peptides and self-DNA in autoimmune skin inflammation. Curr Opin Immunol 2008;20:401–7.
Green DR, Galluzzi L, Kroemer G. Mitochondria and the autophagy-inflammation-cell death axis in organismal aging. Science 2011;333:1109–12.
Hancock REW, Diamond G. The role of cationic antimicrobial peptides in innate host defences. Trends Microbiol 2000;8:402–10.
Hao J, Shen W, Yu G, Jia H, Li X, Feng Z, et al. Hydroxytyrosol promotes mitochondrial biogenesis and mitochondrial function in 3T3-L1 adipocytes. J Nutr Biochem 2010;21:634–44.
Harris TE, Lawrence JC Jr. TOR signaling. Sci STKE 2003;2003:re15–20.
Hunter RL, Dragicevic N, Seifert K, Choi DY, Liu M, Kim HC, et al. Inflammation induces mitochondrial dysfunction and dopaminergic neurodegeneration in the nigrostriatal system. J Neurochem 2007;100:1375–86.
Inoki K, Li Y, Zhu TQ, Wu J, Guan KL. TSC2 is phosphorylated and inhibited by Akt and suppresses mTOR signalling. Nat Cell Biol 2002;4:648–57.
Jacinto E, Hall MN. TOR signalling in bugs, brain and brawn. Nat Rev Mol Cell Biol 2003;4:117–26.
Joven J. Mitochondrial dysfunction: a basic mechanism in inflammation-related non-communicable diseases and therapeutic opportunities. Mediat Inflamm 2013;2013.
Kaminska B. MAPK signalling pathways as molecular targets for anti-inflammatory therapy – from molecular mechanisms to therapeutic benefits. Biochim Biophys Acta-Proteins Proteom 2005;1754:253–62.
Kim I, Rodriguez-Enriquez S, Lemasters JJ. Selective degradation of mitochondria by mitophagy. Arch Biochem Biophys 2007;462:245–53.
Lee HM, Shin DM, Yuk JM, Shi G, Choi DK, Lee SH, et al. Autophagy negatively regulates keratinocyte inflammatory responses via scaffolding protein p62/SQSTM1. J Immunol 2011;186:1248–58.
Möllerström E, Kovács A, Lövgren K, Nemes S, Delle U, Danielsson A, et al. Up-regulation of cell cycle arrest protein BTG2 correlates with increased overall survival in breast cancer, as detected by immunohistochemistry using tissue microarray. BMC Cancer 2010;10:296.
Ma L, Chen ZB, Erdjument-Bromage H, Tempst P, Pandolfi PP. Phosphorylation and functional inactivation of TSC2 by Erk: implications for tuberous sclerosis and cancer pathogenesis. Cell 2005;121:179–93.
Mookherjee N, Brown KL, Bowdish DME, Doria S, Falsafi R, Hokamp K, et al. Modulation of the TLR-mediated inflammatory response by the endogenous human host defense peptide LL-37. J Immunol 2006;176:2455–64.
Morizane S, Yamasaki K, Muhleisen B, Kotol PF, Murakami M, Aoyama Y, et al. Cathelicidin antimicrobial peptide LL-37 in psoriasis enables keratinocyte reactivity against TLR9 ligands. J Investig Dermatol 2012;132:135–43.
Nakahira K, Haspel JA, Rathinam VAK, Lee S-J, Dolinay T, Lam HC, et al. Autophagy proteins regulate innate immune responses by inhibiting the release of mitochondrial DNA mediated by the NALP3 inflammasome. Nat Immunol 2011;12:222, U57.
Nijnik A, Hancock REW. The roles of cathelicidin LL-37 in immune defences and novel clinical applications. Curr Opin Hematol 2009;16:41–7.
Nijnik A, Pistolic J, Wyatt A, Tam S, Hancock REW. Human cathelicidin peptide LL-37 modulates the effects of IFN-gamma on APCs. J Immunol 2009;183:5788–98.
Ong PY, Ohtake T, Brandt C, Strickland I, Boguniewicz M, Ganz T, et al. Endogenous antimicrobial peptides and skin infections in atopic dermatitis. N Engl J Med 2002;347:1151–60.
Park HJ, Cho DH, Kim HJ, Lee JY, Cho BK, Bang SI, et al. Collagen synthesis is suppressed in dermal fibroblasts by the human antimicrobial peptide LL-37. J Investig Dermatol 2008;129:843–50.
Peyssonnaux C, Boutin AT, Zinkernagel AS, Datta V, Nizet V, Johnson RS. Critical role of HIF-1 alpha in keratinocyte defense against bacterial infection. J Investig Dermatol 2008;128:1964–8.
Potter CJ, Pedraza LG, Xu T. Akt regulates growth by directly phosphorylating Tsc2. Nat Cell Biol 2002;4:658–65.
Saitoh T, Fujita N, Jang MH, Uematsu S, Yang B-G, Satoh T, et al. Loss of the autophagy protein Atg16L1 enhances endotoxin-induced IL-1 beta production. Nature 2008;456:264, U68.
Scott MG, Davidson DJ, Gold MR, Bowdish D, Hancock REW. The human antimicrobial peptide LL-37 is a multifunctional modulator of innate immune responses. J Immunol 2002;169:3883–91.
Scott MG, Vreugdenhil ACE, Buurman WA, Hancock REW, Gold M. Cationic antimicrobial peptides block the binding of lipopolysaccharide (LPS) to LPS binding protein. J Immunol 2000;164:549–53.
Takeichi T, Sugiura K, Muro Y, Matsumoto K, Ogawa Y, Futamura K, et al. Overexpression of LEDGF/DFS70 induces IL-6 via p38 activation in HaCaT cells,

similar to that seen in the psoriatic condition. J Investig Dermatol 2010;130: 2760–7.
Wang K, Klionsky DJ. Mitochondria removal by autophagy. Autophagy 2011;7:297–300.
Weichhart T, Costantino G, Poglitsch M, Rosner M, Zeyda M, Stuhlmeier KM, et al. The TSC-mTOR signaling pathway regulates the innate inflammatory response. Immunity 2008;29:565–77.
White E, Karp C, Strohecker AM, Guo Y, Mathew R. Role of autophagy in suppression of inflammation and cancer. Curr Opin Cell Biol 2010;22:212–7.
Wullschleger S, Loewith R, Hall MN. TOR signaling in growth and metabolism. Cell 2006;124:471–84.
Yamasaki K, Di Nardo A, Bardan A, Murakami M, Ohtake T, Coda A, et al. Increased serine protease activity and cathelicidin promotes skin inflammation in rosacea. Nat Med 2007;13:975–80.
Yu J, Mookherjee N, Wee K, Bowdish DME, Pistolic J, Li Y, et al. Host defense peptide LL-37, in synergy with inflammatory mediator IL-1 beta, augments immune responses by multiple pathways. J Immunol 2007;179:7684–91.
Zanetti M. Cathelicidins, multifunctional peptides of the innate immunity. J Leukocyte Biol 2004;75:39–48.
Zhou R, Yazdi AS, Menu P, Tschopp J. A role for mitochondria in NLRP3 inflammasome activation. Nature 2011:475.